Electrophoretic mobility of interacting colloidal spheres

M. Evers, N. Garbow, D. Hessinger, and T. Palberg
Universität Mainz, Institut für Physik, D-55099 Mainz, Germany
(Received 18 August 1997; revised manuscript received 14 January 1998)

The electrophoretic mobility μ of charged colloidal spheres suspended in deionized water was measured as a function of the packing fraction Φ increasing from about 10^{-6} to 2×10^{-3}. With increasing packing fraction, the mobility first increases linearly with the logarithm of the packing fraction and then saturates at a high value unaffected by the freezing transition. The electrostatic potential $\Psi(r)$ was calculated numerically by solving the nonlinearized Poisson-Boltzmann equation in a cell model under conditions of charge regulation. The potential first is constant at low packing fraction and then decreases roughly linearly with $\log(\Phi)$. In both cases the qualitative change in packing fraction dependence occurs once κa significantly (typically 10–20 %) increases above $\kappa_0 a$ given by the residual small ion concentration. Qualitatively similar behavior was found for particles of different size and surface chemistry and also under conditions of added salt. None of the theoretical approaches presently available is able to capture this interesting and complex behavior observed under low salt conditions. [S1063-651X(98)05905-4]

PACS number(s): 82.70.Dd

I. INTRODUCTION

There has been much progress in recent years in the theoretical modeling of electrokinetic properties of isolated colloidal particles. This has been of great interest in industrial applications, where, for instance, stability criteria for concentrated latex dispersions are derived from measurements of the electrophoretic mobility. Also in biological science and medicine, the knowledge of so-called ζ potentials from electrokinetic studies is of importance to understand, e.g., complex transport phenomena in the living organism or to give valuable aid in diagnostics [1]. On the other hand, monodisperse suspensions of charge-stabilized submicrometer spheres became a well-known model system to study the effects of interparticle interactions [2–4]. Typical length scales are on the order of the wavelength of visible light and the structure and dynamics are accessible by light scattering techniques. At sufficiently low concentration of added electrolyte such systems form states of fluid, glassy, or crystalline order much in analogy to atomic matter. The (diffusive) dynamics in these ordered states is observed to be qualitatively different from the single-particle case. Even at low packing fraction, where the effects of hydrodynamic interactions are very small, the long-ranged Yukawa-type interaction and the suspension structure have to be accounted for in calculating the time- and k-dependent collective diffusion coefficients [5]. While the diffusional dynamics are comparably well understood including effects of polydispersity or nonsphericity, there are no such theoretical descriptions for the electrokinetic properties of colloidal spheres in a strongly interacting state. This is mostly due to the lack of reliable and comprehensive experimental data taken of samples under conditions of overlapping electric double layers (EDLs).

The problem of particle interactions and their influence on the electrokinetic properties indeed is fairly complex. Let us make the following assumptions to simplify the situation in an electrophoretic experiment, where the velocity v of a particle is measured in an externally applied electric field E to yield the particle mobility $\mu=v/E$. First, the particles are assumed to be perfectly monodisperse and spherical; a charge is provided by one species of acid surface group that can be characterized by a constant surface pK. Second, the particles are suspended in a 1:1 electrolyte solution, which does not adsorb specifically to the surface. Third, the packing fraction is sufficiently small to neglect hydrodynamic interactions. Even in the case of noninteracting particles we still have to account for the force exerted on a particle by the external electric field, the frictional force, the retardation or electro-osmotic force, and the additional force due to the deformation of the electric double layer, known as electrostriction or relaxation effect. The former three were already incorporated in the theory of Henry [6], while relaxation was included via numerical calculations by Booth [7], Wiersema *et al.* [8], O'Brien and White [9], and others. All those predict a complex dependence of μ on the salt concentration and ζ potential, which is the potential at the so-called plane of shear. The concept of a shear plane approximates the real velocity gradient outward from the surface of a moving particle by geometrically dividing the double layer sharply into one part moving with the particle and one part subject to normal viscous flow. This leads to an effective particle radius a. Unfortunately, there is no general theory as to where this boundary is to be placed, but in most cases it is taken to coincide with either the outer Helmholtz plane or the hydrodynamic radius of the particle as measured by diffusion experiments.

Experimentally, a mobility maximum as a function of added salt is frequently observed for noninteracting particles, the origin of which is still discussed controversially. Here we only briefly mention the ''hairy layer'' concept [10], the site binding model [11–13], the idea of surface conduction [13,14], and interpretation in terms of the high potential solution of O'Brien and White [15]. In addition, careful measurements of ζ potentials by different methods on the same latex often yield different results. In most cases the electrophoretic ζ potential is much smaller than that derived from conductivity increments or calculated from solutions of the Poisson-Boltzmann equation [16]. An overview was recently

TABLE I. Particle properties of the samples investigated. a, geometric radius measured by TEM; a_H, hydrodynamic radius as measured under conditions of added salt by dynamic light scattering; N, number of surface groups as titrated conductometrically; Z, number of dissociated surface groups as calculated numerically for $p\mathrm{K}=0.5$ and $n_P=5\times10^{-16}$ m^{-3}; Z^*_{DH}, Z^*_σ, and Z^*_ζ, effective charges as calculated via a fit of Eqs. (6a) and (6b) to $\Psi(r)$, as derived from conductivity via Eq. (5), and as derived from mobility via Eqs. (1) and (7) with $\Psi_S=\zeta$, respectively. Latex D showed desorption of SDS upon deionizing; numbers given are estimated upper limits as presumably apply for nondeionized condition.

Latex	Batch No.	a (nm)	a_H (nm)	Surface group	N	Z	Z^*_{DH}	Z^*_σ	Z^*_ζ
A	IDC 10-66-58	150.5	154.4±5.3	sulphate	23 100±300	21 400±100	1860±100	2440	1990
B	IDC 10-95-38-202	57.5	62.9±3.5	sulphate	3600±100	3300±50	805±50	730	920
C	A. Weiss PSSL3	35	39.5±2	sulphate	11 800±200	4580±50	570±30	790	495
D	A. Weiss PSL2	51		SDS	<700	<500	<400	<350	<500

given by Hidalgo-Alvarez *et al.* [17].

Working with interacting particles will face two additional problems. First, how are relaxation effects affected in the ordered state, where the (EDLs) overlap significantly? Second, what are the effects of the phase transition from the fluid to the crystalline state? While the effect of increased friction by strongly increased packing fraction has been treated [18], no theoretical answer has been given to date to the electrostatic complications mentioned above. Furthermore, experimental results on strongly interacting lattices differ qualitatively. Okubo presented measurements indicating a significant increase of mobility with decreasing salt concentration followed by a plateau region. He also observed the mobility plateau to be practically independent of both particle size and titrated number of surface groups [19]. Deggelmann *et al.* measured the increase to continue down to salt concentrations of $10^{-7}M$ with apparently only little influence of the packing fraction Φ [20].

In another paper the mobility of cylindrical rods was observed to display a plateau at moderate Φ, but to decrease logarithmically at higher Φ [21]. Such behavior was also observed for deionized suspensions of spheres [22]. However, Bellini *et al.* reported similar measurements performed on a short rod system and found the mobility to first increase but then saturate with increasing Φ [23]. In the same paper they also report on the mobility to decrease with decreasing particle charge. On the other hand, Dunstan and White [24] report pronounced minima in mobility as the packing fraction was reduced at constant low salt concentration. The latter authors and others [16] have pointed out that the cleaning procedures may have significant influence on the measured properties. Keeping in mind that the control of impurities has to be performed at electrolyte concentrations in the micromolar range to stay in the ordered state, preparational differences and difficulties may well explain some of the observed discrepancies.

Recent theoretical considerations of the potential around highly charged colloidal rods and spheres [25–30] yielded numerical procedures to calculate surface potentials and effective interaction potentials that have successfully been applied to the description of phase transitions and diffusional dynamics but have not yet been adapted to electrokinetic phenomena. The mean-field calculations are based on the numerical solution of the nonlinearized Poisson-Boltzmann equation in a spherical Wigner-Seitz cell under conditions of constant charge [27,28] or constant dissociation equilibrium [29]. This yields the highly nonexponential potential $\Psi(r)$, to which a Debye-Hückel-potential $\Psi^*_{\mathrm{DH}}(r)$ is matched at the Wigner-Seitz cell boundary. The corresponding effective charge Z^* is found to be significantly smaller than the true surface charge Z. It is further observed to be on the same order as the effective charges derived from fits of theoretical expressions to data from measurements of the structure factor [20], the phase diagram [31–33], elastic properties [34,35], and conductivity [20,33]. While in the case of interaction-dependent properties this is theoretically well founded (at the position of the nearest neighbor both potentials are indistinguishable) [27,36], the case of electrokinetic properties remains to be clarified.

Systematic measurements on carefully prepared and characterized suspensions are therefore needed to form a comprehensive database to reliably describe the principal qualitative phenomena present in interacting suspensions. The present paper addresses this first step. In the next section we give a detailed description of materials, methods, and preparational procedures used in our study. This is followed by a brief summary of theoretical background needed for data evaluation. We then present experimental data on electrophoretic mobility and conductivity. Results gained at conditions of strong electrostatic interaction are further subjected to comparison with numerically calculated potentials and charge numbers. Finally, possible qualitative explanations of our unexpected results are discussed.

II. SAMPLE PREPARATION AND EXPERIMENTAL METHODS

Two samples (A and B) of commercially available polystyrene latices (IDC, Portland, OR) and two samples (C and D) synthesized and kindly provided by A. Weiss were used. All samples were stabilized by sulphate surface groups stemming from the polymerization initiator and sample D in addition carried a considerable amount of physisorbed sodium dodecylsulphate (SDS) (Merck, Germany). The main features are compiled in Table I.

A and B were shipped at a packing fraction of $\Phi=0.08$ and sample C was at $\Phi=0.055$. From these we prepared stock suspensions of $\Phi\approx0.01$ by dilution with destilled water. Mixed bed ion exchange resin (IEX) (Amberlite UP 604, Rohm and Haas, France) was added and the suspensions were left to stand with occasional stirring for several days. They were then filtered using 0.5-μm filters (Millipore,

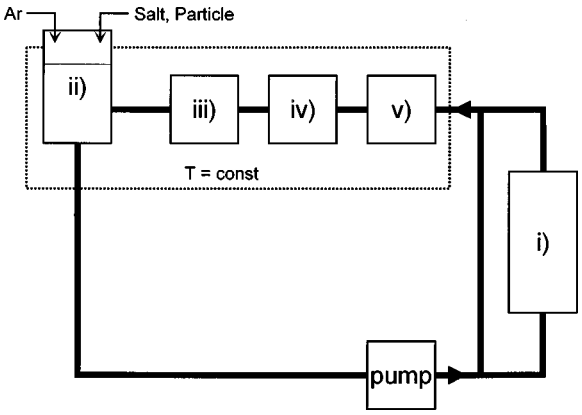

FIG. 1. Block diagram of thermostated closed Teflon tubing system for sample preparation and measurement. Components: (i) ion exchange chamber (bypassed during measurements), (ii) reservoir under inert gas, (iii) laser-Doppler-velocimetry cell, (iv) conductivity measurement, and (v) static light scattering or turbidity measurement. More cells can be added, if necessary. Note the direction of flow.

USA) to remove dust, ion exchange debris, and coagulate regularly occurring upon first contact of suspension with IEX. A second batch of carefully cleaned IEX filled into a dialysis bag was then added to retain low ionic strength in the stock suspensions now kept under Ar atmosphere. Sample *D* was synthesized by standard emulsion polymerization [37] and extensively dialysed against $10^{-3}M$ KCl. Here the stock suspension packing fraction was $\Phi = 0.064$.

All further sample preparation and measurements were performed in a closed system including the measuring cells and the preparational units. Details of the continuous deionization procedures have been given elsewhere [38]. Since preparation may have severe influence on electrophoretic measurements, we nevertheless here give a short outline of the preparational setup as sketched in Fig. 1. The suspension is pumped peristaltically through a Teflon tubing system connecting (i) the ion exchange chamber, (ii) the reservoir under inert gas atmosphere to add further suspension or salt solutions if electrolyte concentration-dependent measurements are performed [14,20], (iii) the observation cell, (iv) a conductivity measurement (electrode LTA01 and bridge WTW 531, WTW, Germany), and (v) a cell for static light scattering or transmission experiments. The latter facilitates an *in situ* control of Φ via the static structure factor or the turbidity. Control of the packing fraction may also be performed via the conductivity at completely deionized conditions (see below). Uncertainties in the packing fraction Φ are typically below 1% at $\Phi = 10^{-3}$. The whole system (excluding the pump) may be thermostated to ± 0.2 °C. During the actual mobility and conductivity experiments the ion exchange chamber is bypassed and great care is taken to ensure stable experimental conditions on a typical time scale of a few hours. Leakage of stray ions into the system was estimated from an increase of the conductivity of pure water (55 nS/cm) of less than 150 nS/cm per hour in the electrophoretic cell to correspond to a NaCl equivalent of $2 \times 10^{-7}M$ h^{-1}. Another source of ionic impurities generally is provided by the particles themselves. The rise in conductivity measured in a suspension is equivalent to the addition of up to $10^{-6}M$ h^{-1} of NaCl.

Before filling the suspension into the tubing system, the latter is rinsed with doubly destilled, filtered water through both the IEX column and the bypass until the eluate shows a conductivity below 60 nS/cm. The volume of water in the tubing system depends on the arrangement of components. It is on the order of 40 cm^3 and is exactly determined by weighing. Then an Ar atmosphere is laid on top of the water surface in the reservoir and stock suspension is added to adjust the desired volume fraction. The suspension is pumped through the ion exchange column for a few hours during which conductivity reaches a constant low value. If desired, then a certain amount of salt is added. A few minutes of further pumping are generally sufficient to reach a constant but higher conductivity value. We note that for each measurement the suspension is deionized again, before a higher amount of salt or further particles are added and the procedure is repeated. We estimate an upper bound for unidentified small ion concentrations during experiments on ''completely deionized'' samples to be between 10^{-7} and $8 \times 10^{-7}M$. Sample *D* also was investigated using this tubing system, again exploiting the possibility to perform several different *in situ* measurements simultaneously on one sample. In this case, however, the sample was not deionized (to prevent desorption of physisorbed tenside [23,33]) but stepwise diluted with $10^{-3}M$ KCl. At such high background electrolyte concentration both leakage of impurities and contribution of desorbing SDS to the ionic strength are assumed negligible.

Electrophoretic measurements were performed in flow through quartz cells of 1×10 mm^2 rectangular cross section (Rank Bros., Bottisham, United Kingdom). In order to avoid the evolution of electro-osmotically caused parabolic flow profiles ac fields of frequencies of 20 Hz and higher are used [39]. The suspension then takes a pluglike flow profile and the measured velocity equals the electrophoretic velocity. The effective electrode separation is on the order of 7 cm and calibrated for each cell by conductivity measurements of 10^{-4}–10^{-1} *M* KCl at 22.5 ± 0.2 °C. Applied fields were between 2 and 70 V/cm. The velocities were found to increase linearly with the applied field strength in all cases and no frequency dependence was observed.

A conventional Doppler velocimetry with real space moving fringe illumination and incoherent detection followed by fast-Fourier-transform frequency analysis (Ono-Sokki, NTD, Japan) was used to determine the electrophoretic velocity. Details of the optics have been given before [39]. Since square wave fields are applied, the resulting spectra contain a convolution of the velocity distribution with a sequence of δ peaks at multiples of the ac-field frequency. For evaluation we follow the method of Uzgiris, which is discussed in detail elsewhere [40]. Here we only note that the determination of the Doppler shift is limited in accuracy to half the ac-field frequency. Under our experimental conditions this results in a typical upper bound for the residual uncertainties in μ on the order of 10%.

III. PACKING FRACTION DEPENDENCE OF ELECTROPHORETIC MOBILITIES

Theoretical expressions for the electrophoretic mobility μ have been available since the start of the century for the

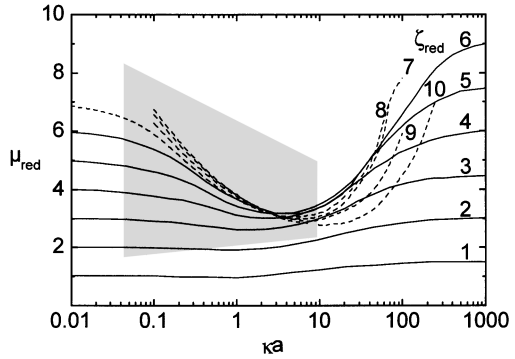

FIG. 2. Comparison of theoretical predictions for the reduced electrophoretic mobility for several values of the reduced ζ potential and varying κa with the range of experimental results (shaded area). Predicted mobilities after [8,9] (including relaxation effects) are shown by the solid and dashed lines, respectively. Note that a significant portion of experimental results is not accounted for by theory.

limiting cases of very thin and very thick EDLs [41,42]. Taking into account retardation effects, Henry's formula [6] gives a prediction for the mobility over a much wider range of experimental parameters:

$$\mu=\frac{2\varepsilon\varepsilon_0\zeta}{3\eta}\left[1+\frac{(\kappa a)^2}{16}-\frac{5(\kappa a)^3}{48}-\frac{(\kappa a)^4}{96}+\frac{(\kappa a)^5}{96}+\left(\frac{(\kappa a)^4}{8}-\frac{(\kappa a)^6}{96}\right)\exp(\kappa a)\int_{\infty}^{\kappa a}\frac{\exp(-t)}{t}\,dt\right], \quad (1)$$

where $\varepsilon\varepsilon_0$ is the dielectric permittivity κ^2 of water, η the suspension viscosity, a the particle radius, and κ the Debye-Hückel screening parameter defined via

$$\kappa^2=\frac{e^2}{\varepsilon\varepsilon_0 k_B T}\sum_i n_i z_i^2, \quad (2)$$

with the thermal energy k_BT, the elementary charge e, the number density n_i, and the valence z_i of small ions of all species i in the suspension. This expression is valid for arbitrarily large ζ potentials and interpolates between the expressions derived by Hückel and by von Smoluchowski for the limits of $\kappa a \ll 1$ and $\kappa a \gg 1$, respectively.

Later on also relaxation effects were included in the theoretical expressions and several authors provided numerical solutions for isolated particles [7–9]. For small ζ potentials the predictions of Wiersema *et al.* are shown in Fig. 2 in terms of the reduced quantities

$$\mu_{\mathrm{red}}=\frac{2}{3}\frac{\eta}{\varepsilon\varepsilon_0 k_B T}\mu, \quad \zeta_{\mathrm{red}}=\zeta\frac{e}{k_B T}. \quad (3)$$

We also include the predictions of O'Brien and White for large potentials ($\zeta_{\mathrm{red}}\geqslant 7$) and their upper bound for the mobility as a function of κa. Curves for $\zeta_{\mathrm{red}}>3$ show a minimum around $\kappa a\approx 1-10$, which deepens with increasing ζ. This is due to the relaxation effect, i.e., the distortion of the EDLs in the presence of an external field leading to a significantly smaller local field strength. In particular, an upper bound of mobilities $\mu_{\mathrm{red}}\leqslant 4$ for $0.5\leqslant\kappa a\leqslant 20$ is predicted.

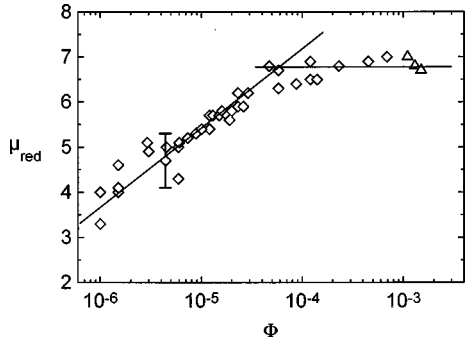

FIG. 3. Packing-fraction-dependent reduced electrophoretic mobility of sample *A* under conditions of no added salt (residual stray ion concentration well below $10^{-6}M$). The straight lines are guides to the eye. The reproducibility of a single measurement is given by the error bar. As Φ is increased over more than two orders of magnitude $\mu(\Phi)$ first increases linearly with the logarithm of the packing fraction and reaches a plateau value of $\mu_{\mathrm{red}}=6.8\pm 0.3$ for $\Phi>5\times10^{-5}$. The triangles correspond to the mobility in the crystalline state. For all other points of the plateau we observe pronounced fluid order.

Some experimental evidence of this behavior has recently been given [43], but unfortunately the authors did not quantify their ''very low'' packing fractions. We further note that these theories form the basis of standard evaluation procedures, even while significant deviations from predicted values have been observed experimentally.

Comparing our measurements with these theories, we observe a significant portion of data to be way outside the allowed range of mobilities. Much too large mobilities have been reported before, but with qualitative differences in the functional form of the Φ dependence [20–23]. These results cannot be explained by the standard electrokinetic model.

Figure 3 shows the results of a measurement on sample *A* at deionized conditions plotted versus the decadic logarithm of the packing fraction. Starting from a value of $\mu_{\mathrm{red}}=3.3$, the mobility increases linearly with $\log(\Phi)$ and becomes almost independent on Φ for $\Phi>5\times10^{-5}$ with a saturation value of $\mu_{\mathrm{red}}=6.8\pm0.4$. For small packing fractions the observed mobilities are well below the predictions, while they are well above for large Φ. It is interesting to note that the crossover in qualitative behavior (increase versus constancy) coincides with the range of concentrations where the fluidlike order evolves. At very low values of the packing fraction the particles may be considered as noninteracting in the sense that the suspension structure is isotropic [$S(k)=1$], while at higher concentration the sample forms a fluidlike order and crystallizes for $\Phi\geqslant 9\times10^{-4}$. Data points of the crystalline phase are given by the triangles. Within experimental error, however, there is little, if any, influence of the phase transition. On the other hand, we observe the crossover at the packing fraction, where the concentration of ions provided by the particles ($2\times10^{-7}M$ from the dissociation product of water) is significantly increased above the concentration of ions provided by the suspending medium.

An interesting question now is whether this behavior is qualitatively reproducible, i.e., independent of the surface chemistry of the latex and of its size. Figure 4 compares the packing fraction dependences for all our samples. Using real fringe and incoherent detection, the signal-to-background ra-

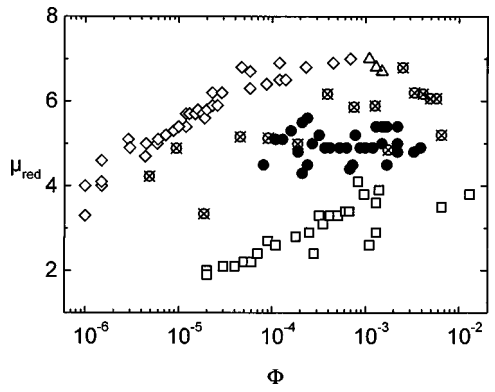

FIG. 4. Same as Fig. 2 for all samples. ◇, sample *A*, fluid; △, sample *A*, crystalline; ⊗, sample *B*, ●, sample *C*; □; sample *D*. Note that no decrease of mobility with increasing packing fraction is observed.

tio is generally smaller for smaller particles at the same packing fraction. Data were taken at different ranges, thus covering more than four orders of magnitude of Φ. We note that restrictions of the range of accessible packing fractions are given by a low signal-to-noise ratio at low packing fractions and the onset of multiple scattering at high Φ and thus depend on the individual scattering length of the particles. The individual values of the mobilities vary significantly, reflecting the different particle properties. More importantly, clear common trends in the functional form of the Φ dependence may be derived.

Although with considerably larger scatter sample *B* shows the same qualitative behavior, namely, first an increase in $\mu_{\rm red}$ with log(Φ) and a crossover to independence of the packing fraction as the concentration of counterions is on the same order as the concentration of ambient electrolyte. As can be noticed from Fig. 5, the mobility of deionized suspensions crucially depends on the background level of stray ions. In fact, the value may drop more than a factor of 2 if some μM are reached. The scattering of data for sample *B* was caused by a small leak in the lid of the reservoir, which has to be lifted to add particles or salt. For sample *C*

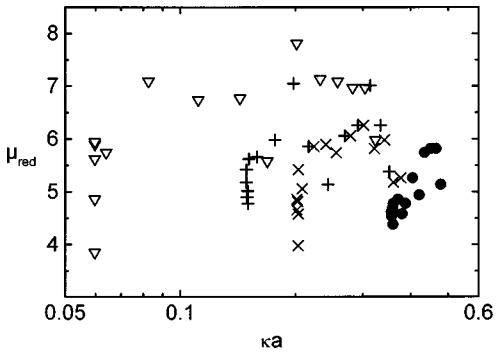

FIG. 5. Packing-fraction-dependent reduced electrophoretic mobility of sample *B* under conditions of small amounts of added salt plotted versus κa as calculated from Eq. (4). The symbols denote the following concentrations of added NaCl: ▽, $c=0\ \mu M$; +, $c=0.5\ \mu M$; ×, $c=0.8\ \mu M$; ●, $c=1.3\ \mu$M. All curves show qualitatively similar behavior, i.e., a tendency to saturate as κ is increased. The crossover point in all samples coincided with the evolution of fluid order.

the counterion concentration exceeds the concentration of added salt. Here the mobilities show a pronounced plateau for all packing fractions investigated.

Measurements on sample *D* were performed at constant salinity of $10^{-3}M$ KCl. This value is large enough to safely neglect the contribution of particle counterions to κ. While κa thus is constant, we again observe a continuous rise of μ with the packing fraction increasing from 2×10^{-5} to 10^{-2}. For $\Phi\geqslant8\times10^{-4}$ the determined mobility is well outside the range covered by theories for single particles including relaxation. For $\Phi\leqslant5\times10^{-3}$ the concentration of added salt ions greatly exceeds the concentration of counterions and the plateau region is not completely reached. Nevertheless, the increase in mobility is less pronounced for the high-packing-fraction values, possibly indicating the beginning of saturation.

We further performed measurements on sample *B* at various concentrations of added electrolyte each over a large range of Φ. We plot the results versus κa with κ calculated as

$$\kappa=\sqrt{\frac{e^2}{\varepsilon\varepsilon_0 k_B T}\,(nZ^*+2\times1000N_A c)}. \tag{4}$$

The first term in the sum of Eq. (4) considers the contribution of the particles via the effective number of counterions Z^* and the number density of particles $n=3\Phi/4\pi a^3$; N_A is Avogadro's number and c is the molar concentration of added 1:1 electrolyte. Z^* may be calculated (see below) or determined experimentally, e.g., from the packing-fraction-dependent conductivity measurement. Consistent with previous experiments [20,34], here also the conductivity of samples *A*, *B*, and *C* in the ordered state was observed to be linear in Φ and to follow the expression

$$\sigma=eZ_\sigma^* n(\mu_P+\mu_+)+\sigma_{\rm H_2O}, \tag{5}$$

where the suffix σ denotes the measurement of Z^* via conductivity, μ_P is the measured particle mobility, and μ_+ is the counterion mobility, which in this case is given by $\mu_{\rm H^+}=36.2\times10^{-8}\ {\rm m^2\,V^{-1}\,s^{-1}}$ for the protons. $\sigma_{\rm H_2O}=55$ nS/cm denotes the background conductivity of water. Equation (5) assumes independent migration of all ions with their bulk mobilities. Any interaction effects between particles and small ions are accounted for in the effectively transported counterion number or effective transport charge number Z_σ^*, which is more than an order of magnitude smaller than the number of dissociated surface groups, the bare charge number Z, and only slightly different from the numerically calculated effective charge $Z_{\rm DH}^*$ (see below).

Using Z_σ^* in Eq. (4), we calculate κa and plot the mobilities of sample *B* in Fig. 5. The uppermost curve was taken at deionized conditions. Plotted this way, the coincidence of the crossover region with the equality of counterion and background concentration is even more pronounced. The slope of the curve changes from nearly vertical as κ is dominated by the (constant) background electrolyte to nearly horizontal, as κ starts to be influenced by the counterion concentration. As compared to the data taken at deionized conditions, the curves at low concentrations of added electrolyte show a significantly worse statistical quality. This is due to the fact

that the amounts of added salt are on the order of the concentrations of stray ions that may enter upon opening the reservoirs to add the salt. Nevertheless, for all curves a qualitatively similar behavior is observed.

We summarize our experimental findings as follows. Starting from a noninteracting suspension [in the sense of $S(k)=1$], where mobilities are smaller than predicted, the increase of the packing fraction leads first to a logarithmic increase in mobility. Parallel to the starting overlap of EDLs and the corresponding evolution of fluid order, the mobility then saturates at a value much larger than allowed by the theories of [7–9]. We further note that the observed systematic packing-fraction dependence of the mobility is in complete disagreement with the predictions of [18]. The observed crossover from a logarithmic increase to saturation seems to be a very general feature of colloidal particles irrespective of surface chemistry, size, and possibly also of their form. It occurs once the concentration of counterions is on the order of or exceeds the concentration of added or underlying salt.

Our unexpected results are supported by some of the earlier measurements of other authors. The data of Bellini *et al.* on short charge variable rods show an increase of mobility with Φ at low packing fraction and a constant mobility at large Φ. Also, the experiments reported by Deggelmann *et al.* were performed at very-well-defined experimental conditions. There, both for long rods (tabac mosaic virus) [21] and for spherical particles [20,22] a constant high mobility was observed for moderate packing fractions and under deionized conditions. For highly charged 100-nm spheres and $\Phi \leqslant 10^{-4}$ the plateau value of the mobility was $\mu = 20 \times 10^{-8}\ \mathrm{m^2\,V^{-1}\,s^{-1}}$. If, in view of our results and those of Bellini *et al.*, one assumes the counterion concentration to exceed the concentration of added salt already at low Φ, the result compares well with our data on sample *C*.

At larger packing fraction, however, a *decrease* of mobility with increasing Φ was found for both spheres and long rods, which is not present in our data on moderate volume fractions. The onset of the decrease shifted towards higher Φ upon adding salt.

IV. COMPARISON OF MEASUREMENT AND NUMERICAL CALCULATIONS

In the next step we will compare numerically calculated surface potentials to ζ potentials derived from experimental mobilities via several approaches. To calculate the electrostatic potential $\Psi(r)$ of a highly charged spherical particle with radius a in the diffuse part of the EDL, i.e., outside the Stern layer, one has to numerically solve the nonlinearized Poisson-Boltzmann (PB) equation. Following the suggestions of Alexander *et al.* [28], the PB equation is solved self-consistently in a spherical Wigner-Seitz cell of radius r_{WSZ} given by the particle density to yield $\Psi(r)$. For low charge Z and large particles this mean-field approximation has recently been shown to nearly quantitatively reproduce results from primitive model calculations [27,30].

In order to have a tractable analytic expression a so-called Debye-Hückel potential is then fitted to the numerical solution

$$\Psi_{\mathrm{DH}}(r) = \Psi_S \frac{a}{r} \exp[-\kappa(r-a)], \tag{6a}$$

with

$$\Psi_S = \Psi_{\mathrm{DH}}(a) = \frac{Ze}{4\pi\varepsilon\varepsilon_0} \frac{1}{(a+\kappa a^2)} \tag{6b}$$

being the surface potential. Note that Eq. (6a) reduces to a Yukawa potential in the limit of vanishing a. Upon adding a suitable van der Waals term the celebrated Derjaguin-Landau-Verwey-Overbeek potential for a pair of isolated spheres is recovered.

A fit of Eq. (6a) to this solution with κ calculated from the exact concentrations at the cell boundary and subsequent integration from the cell boundary up to the surface yields an effective charge number Z^*_{DH} replacing the much larger analytical or bare charge Z in Eq. (6b). After [28], Z^*_{DH} has become known as the renormalized charge and was successfully employed to describe different interaction-dependent properties such as phase behavior [36], phase transition kinetics [32], the structure of binary mixtures [44], the elasticity of colloidal crystals [34,35], and diffusive dynamics [45]; the concept is therefore widely accepted, but has not been shown to apply for electrokinetic phenomena.

Here we use a program kindly provided by Belloni [29] that in addition accounts for the surface chemistry of the particles through fixing the surface pK instead of Z. Due to the accumulation of counterions in the surface region of the particle, the surface pH may be significantly lowered and thus alter the degree of dissociation when it becomes comparable to the surface pK. The PB equation is thus solved under conditions of charge regulation and with ε, T, c, Φ, a, and N as input the program yields Z, Z^*_{DH}, and $\Psi(r)$ as output. Since the effective potential $\Psi_{\mathrm{DH}}(r)$ is not directly accessible from the program it is calculated using Z^*_{DH}, and Eq. (4) for κ in Eqs. (6a) and (6b). In Fig. 6 we present the numerical results for the reduced potential $\Psi(r)$, reduced effective potential $\Psi_{\mathrm{DH}}(r)$, and bare and effective charges Z and Z^*_{DH} of latex *A* as a function of packing fraction at no added salt. The stray ion concentration was assumed to be $10^{-7}M$ of a neutral 1:1 electrolyte. The effective potential is significantly smaller than the true surface potential. The effective charge is one order of magnitude smaller than the bare charge, which in turn is slightly smaller than the number of surface groups N over practically the whole experimental range. Only at increased Φ the true surface charge Z approaches N; at even larger Φ an increase in Z^*_{DH} towards Z is observed [46].

Concerning our mobility results, the most interesting point is Φ dependence of the potentials. Both potentials stay practically constant up to $\Phi \approx 10^{-3}$ and then decrease with the logarithm of Φ. It is interesting to note that this crossover in qualitative behavior appears as the concentration of counterions nZ^*_{DH}/N_A at r_{WS} increases above the average background concentration c of small ions. As the distance between particles decreases with increasing Φ, this corresponds to the region where the influence of neighboring particles on the potential around a given particle becomes obvious in the numerical calculations.

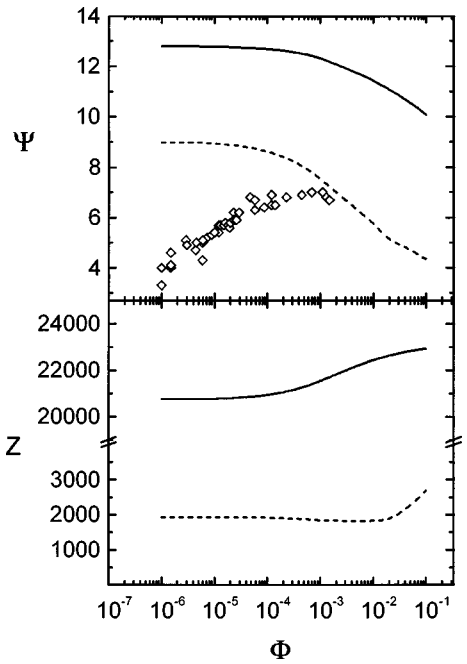

FIG. 6. Top, comparison of numerically calculated surface potentials $\Psi(r)$ (——) and effective surface potentials $\Psi^*_{\mathrm{DH}}(r)$ (− − −) with ζ potentials as derived from measured mobilities via Eq. (1) (◇); bottom, numerical calculations of the corresponding charge numbers. Note that while the degree of dissociation increases with increasing Φ, the effective charge (− − −) goes through a minimum before approaching the bare charge (——).

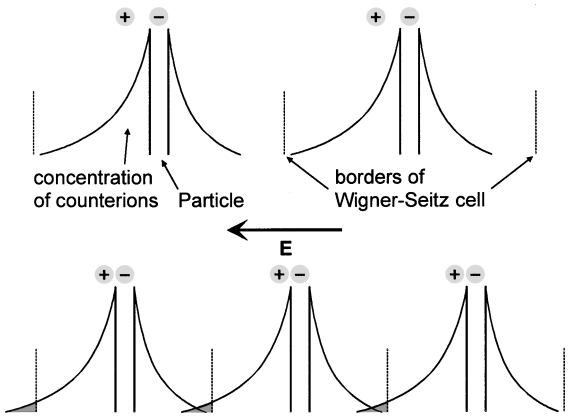

FIG. 7. Qualitative sketch of the relaxation effects present under conditions of isolated particles (top) and of overlapping EDLs (bottom). Shown is the radial ion concentration parallel to an applied electric field E. Note the distortion present for isolated particles. The presence of neighboring particles increases the concentration of counterions near the Wigner-Seitz cell boundary. At increasing overlap the drift of counterions away from the particle is increasingly compensated by those arriving from neighboring particles. As a consequence, relaxation effects should vanish upon increasing the packing fraction.

To quantitatively compare our experimental data with numerical determined potentials or charge numbers we have to convert the mobilities into the corresponding ζ potential. As stated before, several possibilities are available. Evaluation of our data following [8,9] in the low-packing-fraction regime yields an increasing ζ potential starting from $\zeta_{\mathrm{red}}=3.6$ at the lowest packing fraction. This is in obvious disagreement with the potential calculations. Qualitatively, a constancy of the ζ potential is expected. Quantitatively, the value of the ζ potential at $\Phi=10^{-6}$, where the standard electrokinetic model should actually apply, is a factor of 3 too low. An evaluation after Eq. (1) does not alter this result.

Above $\Phi=2\times10^{-5}$ where $\zeta_{\mathrm{red}}>10$, no evaluation after this standard procedure is possible. Thus our experimental result seems to be in both qualitative and quantitative disagreement with the numerical predictions of [8,9].

This is in line with previous experiments of other groups. While measurements of the ζ potential via the conductivity increment seem to yield results compatible with numerical calculations of the surface potential, much too low values for the salt-concentration-dependent mobility and consequently also small potentials have been observed previously [14,16,19] for noninteracting particles in the sense of $S(k)=1$. On the other hand, Deggelmann *et al.* [20] reported mobilities above these predictions for ordered systems.

An evaluation after Eq. (1) [6] not considering any relaxation effects yields potentials first strongly increasing with Φ but showing a nearly constant value of $\zeta_{\mathrm{red}}=6.8$ for $\Phi\geqslant2\times10^{-5}$. This value and the corresponding charge number of 1990 are well below the numerical values of $\Psi(a)\approx12$ and $Z=21\,400$ ($\Phi=7\times10^{-4}$). Interestingly, both the potential and charge number approach the effective surface quantities predicted numerically. This also is the case for samples *B* and *C* at the same particle number density (cf. Table II). We note, however, the qualitative disagreement: The experimentally determined potential increases where the numerical calculation predicts a constant value, but remains constant where Ψ decreases. Therefore, at present we cannot verify the applicability of charge renormalization in electrophoretic experiments.

We summarize our findings as follows. The mobility increases where the potentials are constant, while it is essentially constant where the potentials decrease. The crossover region spans roughly a decade in packing fraction.

V. VANISHING RELAXATION EFFECTS

It is tempting to speculate that the plateau observed in ζ for $\Phi>2\times10^{-5}$ is due to the compensation of two effects: For constant potential the mobility shows a logarithmic increase with packing fraction; the potential, however, begins to decrease logarithmically for $\Phi>2\times10^{-5}$ compensated by a decrease in potential. A possible reason for a mobility increase could be the vanishing of relaxation effects with increasing packing fraction.

This qualitative picture is conceptually straightforward and may provide a starting idea to quantitatively incorporate many-particle effects into the calculation of electrophoretic mobilities. It is sketched in Fig. 7. Consider the EDL surrounding an isolated particle suspended in an infinite reservoir of suspending water. The EDL in principle extends to infinity too. In practice, the excess counterion concentration is negligible as compared to the bulk concentration of background electrolyte after a few micrometers. Distortions of the EDL due to the applied electric field occur undisturbed by neighboring particles or walls.

Adding more particles to the system, the EDL extension is

TABLE II. Comparison of possible positions of the shear plane given in nanometers and the corresponding reduced potentials from different experimental methods and criteria (the calculated data are based on a particle density $n_P = 5 \times 10^{-16}$ m^{-3}).

Latex	a (nm)	$\Psi(a)$	$\Psi_{\mathrm{DH}}(a)$	a_H (nm)	$\Psi_{\mathrm{DH}}(a_H)$	a_ζ (nm)	ζ_{red}	a_σ (nm)	$\Psi(a_\sigma)$	a_{kT} (nm)	$\Psi(a_{kT})$
A	150.5	12.4	7.8	154.4	7.6	186	6.8	194	6.3	655	1.0
B	57.5	12.6	9.7	62.9	8.8	86	6.7	95	5.8	399	1.0
C	35.0	15.4	11.4	39.5	9.9	68	5.8	414	0.6	305	1.0

decreased. A sensible estimate may be the Wigner-Seitz cell boundary. This must not yet lead to electrostatic repulsion between particles and to structure formation. Distortions of the EDL, however, upon applying an electric field now might become heavily altered. We note that strong deviations of experimental data from theoretical predictions are found exactly in this regime.

Adding more and more particles, the EDL of one particle, i.e., the region of deviations from electroneutrality, may start overlapping significantly into the neighboring Wigner-Seitz cell. Thus the charge separation occurring for a single particle due to the drift of small ions away from the surface is (partially) compensated by small ions arriving from the opposite direction. Consequently, the relaxation effects observed at infinite dilution (and possibly enhanced at moderate concentrations) should decrease as the packing fraction is increased. Returning to Figs. 3–5, the crossover is observed as the counterion concentration exceeded the residual small ion concentration by some 10–20 %, giving an estimate for the start of EDL overlap. While at constant potential this will lead to an increase in mobility, a decreasing potential will compensate the effect. Our model may therefore qualitatively explain the observed trends.

In the case of a strongly overlapping EDLs combined with a high packing fraction the relaxation effects may even vanish completely. In that case the mobility again should follow the qualitative behavior of the potential. In fact, Deggelmann [22], who used the same preparational methods as presented in the present paper, observed a plateau for the mobility of particles with $a = 50$ nm followed by a logarithmic decrease for $\Phi > 6 \times 10^{-5}$. In view of our speculation, this result would correspond to the high-packing-fraction end of a general Φ-dependent mobility.

A similar picture may apply to the salt concentration dependence. Both Okubo [19] and Garbow [14] report a low mobility plateau with decreasing salt concentrations $c \leqslant 10^{-4} M$. Mobilities measured by Deggelmann [20] show first the well-known maximum at moderate c, then a minimum at lower c, followed by a steep increase coinciding with the evolution of fluid structure as c is further decreased. In this view the important feature would be the minimum corresponding to the onset of vanishing relaxation in samples with sufficiently high packing fraction. Consequently, the notion of noninteracting particles should, for electrokinetic experiments, be reconsidered and possibly redefined in terms different from structural criteria.

Being far from presenting a quantitative theoretical treatment, here we could only offer a qualitative interpretation in terms of vanishing relaxation. We note that this qualitative sketch of the situation as drawn in Fig. 7 does not yet include complications due to the formation of fluidlike order nor does it have an explanation for the functional form of the mobility increase. It may, however, outline a possible road for the development of theoretical descriptions.

VI. THE SHEAR PLANE CONCEPT

This question is even more complex to treat and we may only give some considerations concerning the position of the shear plane derived from different measurements that might illustrate the problem rather than solve it. We will discuss sample *A* in detail and give a compilation of results in Tables I and II. In Fig. 8 we show the numerical solutions for the radial counterion distribution and the true potential $\Psi(r)$ as obtained for latex *A* at no added salt and strongly overlapping EDLs where sample *A* showed a pronounced fluid order. We first discuss possible positions of the shear plane while assuming the concept to apply also for ordered samples and then address an obvious limitation of this concept.

We recall that the concept of a shear plane approximates the real velocity gradient outward from the surface of a mov-

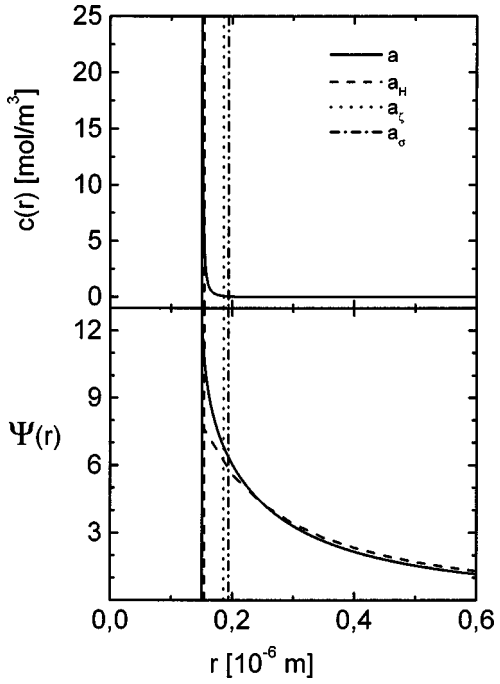

FIG. 8. Top, radial counterion distribution; bottom, mean-field potential as calculated for a particle of sample *A* with a geometrical radius of 150.5 nm at no added salt (residual stray ion concentration $10^{-7} M$) and packing fraction $\Phi = 0.0007$ (——) and the potential Ψ_{DH} (— — —) approximated via Eq. (6a). The vertical lines indicate possible positions of the plane of shear as derived from geometrical radius a (SLS), hydrodynamic radius a_H (DLS), and conductivity a_σ compared to a_ζ as derived from the measured ζ potential.

ing particle by geometrically dividing the double layer sharply into one part moving with the particle and one part subject to normal viscous flow. Traditionally, two positions of the shear plane are discussed. One of them is the Stern layer boundary. In our case of the absence of specific absorption the Stern layer is empty. Hence, this layer contains no charge; neglecting its thickness, the shear plane coincides with the geometrical radius $a=150.5$ nm as determined from static light scattering.

Alternatively, many authors assign the value of the hydrodynamic radius a_H to the position of the shear plane. We note that the hydrodynamic radius replacing the geometrical radius in experiments on the self-diffusion also is derived from a similar concept. We determined $a_H=154.4$ nm from dynamic light scattering performed on very dilute samples in the limit $\kappa a \gg 1$, where large amounts of added salt suppress the particle interaction. In agreement with previous experiments, we observe a_H to be only slightly larger than a for all samples.

A third possibility exploits the results of the conductivity experiment. There we found that only an effective number Z_σ^* of counterions is transported with their bulk mobilities. A physical interpretation would be that close to the particle transport is hindered by either the strong interaction of the ions with the particle or a hairy layer [47], both leading to an enhancement in the viscosity and/or a reduction of small ion mobility close to the surface. In Eq. (5) this presumably smooth variation [47–49] again is approximated by a steplike increase in small ion mobility at a radius a_σ. We therefore vary the upper boundary of the integral over the excess counterion concentration

$$Z=\int_{r_{\mathrm{WS}}}^{a_\sigma} c(r)-c(r_{\mathrm{WS}})r\ dr \tag{7}$$

until Z equals Z_σ^* to obtain $a_\sigma=194$ nm.

One may also try a naive energetic criterion. Following the picture of counterion condensation one might argue that if the external field is very small, only ions bound by less than k_BT should be able to move relatively to the colloidal particle. The radius derived from this criterion $\Psi(r)=1$ is $a_{kT}=655$ nm.

Finally, these four values are compared with the position of the shear plane as derived from the electrophoretic mobility. Referring to Fig. 6, the ζ potential in the plateau region was obtained to be $\zeta_{\mathrm{red}}=6.8$. This corresponds to a shear plane radius of $a_\zeta=186$ nm if the solution to the nonlinearized PB equation is taken as the true potential. Figure 8 gives a comparison of all values obtained for sample A, except the $1k_BT$ criterion, which gives an unphysical position of the shear plane much too far from the surface to explain the observed high mobility values.

For sample A the conductivity radius yields a position of the shear plane very close to the value derived from mobility. The hydrodynamic radius as measured at added salt is significantly smaller and much closer to a. This can be understood by taking into account the hairy layer concept. Within the range of our equipment we could not measure the hydrodynamic radius under conditions of complete deionization. We note, however, that measurements performed by single-particle tracking on a variety of particles including sample A at $\Phi\approx 10^{-7}$ and under conditions of saturation with CO_2 but no salt added [50] indicate a significant increase of a_H as compared to a.

Systematic measurements on this point have recently been performed by Seebergh and Berg [47]. They observed the hydrodynamic radius of noninteracting particles to increase with decreasing salt concentration. The effect was not present if the particles were heat treated and it was attributed to the presence of a hairy layer on the particle surface. As those dangling ends carry the ionogenic surface groups they will stretch out as the screening is reduced. An immobilized water layer results, which may extend several nanometers into the surrounding fluid. For sample A both the coincidence of a_σ and a_ζ and the disagreement as compared to a_H at large salt concentration may thus possibly be explained by the presence of hairs on the particle surface. While for sample B the situation is similar, radii derived for the more highly charged sample C show a clear disagreement between the respective possibilities to position the shear plane. Clearly additional precise experiments on particle radii at deionized conditions are needed to further comment on this point. At present we can only state that a_H as measured under added salt seems to provide a questionable approximation for the position of the plane of shear under conditions of no added salt and strong overlap of EDLs, respectively.

VII. CONCLUSIONS

We presented systematic measurements on the packing-fraction-dependent mobility of strongly charged colloidal spheres showing a pronounced and complex influence of double-layer overlap on the electrokinetic properties. First, we found an unexpected increase of the mobility with increasing packing fraction that cannot be explained within the standard electrokinetic model. It is also incompatible with theoretical predictions taking into account increased hydrodynamic interaction. No influence of the phase transition into the crystalline ordered state was detected. Further, an increase in mobility was observed, where the calculated surface potentials remain essentially constant and are followed by a crossover to constant mobility as the potential starts to decrease. Using Henry's theory this behavior translates to a similar phenomenology for the ζ potential. We suggested the vanishing of relaxation effects in combination with a decrease in surface potential to be a possible explanation.

Second, the crossover was observed to occur when the concentration of counterions at the Wigner-Seitz cell boundary starts to significantly exceed the concentration of underlying electrolyte. Alternatively to the evolution of fluid order, this could be taken as a criterion for the onset of particle interaction.

Third, an unexpected closeness of ζ and the effective surface potential $\Psi_{\mathrm{DH}}^*(a)$ was observed for a number of samples. At first sight this may suggest a consistent description of electrokinetic and other interaction-dependent properties in terms of the renormalization concept. Our finding, however, has to be rated fortuitous until further measurements covering also significantly higher packing fractions possibly confirm a systematic decrease in μ and ζ, respectively. At present we are not aware of any physical reason why the ζ potential at the shear plane as determined by elec-

trophoresis should equal an effective surface potential. Clearly, a theory of electrokinetic properties in strongly interacting colloidal suspensions remains a challenge.

Finally, the position of the shear plane derived from a comparison of the ζ potential to the numerical calculated $\Psi(a)$ and also from conductivity is found to be some 20 nm above the particle surface. A possible explanation would be the assumption of hairy layers stretching out with decreasing salt concentration. While this probably is an effect independent of the particle interaction and thus should not be held responsible for the general trend of Φ-dependent mobilities, it may nevertheless be responsible for the particular plateau values of μ.

ACKNOWLEDGMENTS

It is a pleasure to thank L. Belloni, B. Weyrich, and H. Löwen for instructive discussions and numerical support. The authors gratefully acknowledge financial support from the Materialwissenschaftliches Forschungszentrum, Mainz and the Bundesministerium für Forschung und Technik.

[1] R. J. Hunter, *Zeta-Potential in Colloidal Science* (Academic, London, 1981).
[2] P. N. Pusey, in *Liquids, Freezing and Glass Transition*, Proceedings of the Les Houches Summer School of Theoretical Physics, Les Houches, 1989, edited by J. P. Hansen, D. Levesque, and J. Zinn-Justin (Elsevier, Amsterdam, 1991), p. 763.
[3] R. Klein, in *Structure and Dynamics of Strongly Interacting Colloids and Supramolecular Aggregates in Solution*, Vol. 369 of *NATO Advanced Study Institute, Series C: Mathematical and Physical Sciences*, edited by S.-H. Chen, J. S. Huang, and P. Tartaglia (Kluwer, Dordrecht, 1992), p. 39.
[4] *Physics of Complex and Supramolecular Fluids*, edited by S. A. Safran and N. A. Clark (Wiley-Interscience, New York, 1987).
[5] G. Nägele, Phys. Rep. **272**, 217 (1996).
[6] D. C. Henry, Trans. Faraday Soc. **44**, 1021 (1948).
[7] F. Booth, Proc. R. Soc. London, Ser. A **203**, 514 (1950).
[8] P. H. Wiersema, A. L. Loeb, and J. T. G. Overbeek, J. Colloid Interface Sci. **22**, 78 (1966).
[9] R. W. O'Brien and L. R. White, J. Chem. Soc., Faraday Trans. 2 **74**, 1607 (1978).
[10] A. G. Van der Put and B. H. Bijsterbosh, J. Colloid Interface Sci. **92**, 499 (1983).
[11] C. F. Zukoski and D. A. Saville, J. Colloid Interface Sci. **114**, 32 (1986).
[12] C. F. Zukoski and D. A. Saville, J. Colloid Interface Sci. **114**, 45 (1986).
[13] L. P. Voegtli and C. F. Zukoski, J. Colloid Interface Sci. **141**, 92 (1991).
[14] N. Garbow, Ph.D. thesis, Universität Mainz, 1996 (unpublished), p. 113ff.
[15] M. Antonietti and L. Vorwerg, Colloid Polym. Sci. **275**, 883 (1997).
[16] B. R. Midmore and R. J. Hunter, J. Colloid Interface Sci. **122**, 521 (1988).
[17] R. Hidalgo-Alvarez, A. Martin, A. Fernandez, D. Bastos, and F. J. de las Nieves, Adv. Colloid Interface Sci. **67**, 1 (1996).
[18] S. Levine and G. H. Neal, J. Colloid Interface Sci. **47**, 520 (1974).
[19] T. Okubo, Ber. Bunsenges. Phys. Chem. **92**, 504 (1988).
[20] M. Deggelmann, T. Palberg, M. Hagenbüchle, E. E. Maier, R. Krause, Chr. Graf, and R. Weber, J. Colloid Interface Sci. **143**, 318 (1991).
[21] M. Deggelmann, Chr. Graf, M. Hagenbüchle, U. Hoss, Chr. Johner, H. G. Kramer, Chr. Martin, and R. Weber, Phys. Chem. **98**, 364 (1994).
[22] M. Deggelmann, *Elektrophoretische Lichtstrenung als Sonde zur Untersuchung Makromolekularer Suspensionen* (Hartung-Gorre, Konstanz, 1992).
[23] T. Bellini, V. Degiorgio, F. Mantegazza, F. A. Marsan, and C. Scarneccia, J. Chem. Phys. **103**, 8228 (1995).
[24] D. E. Dunstan and L. R. White, J. Colloid Interface Sci. **152**, 297 (1992).
[25] G. S. Manning, J. Chem. Phys. **51**, 924 (1951).
[26] L. Belloni, M. Drifford, and P. Turq, Chem. Phys. **83**, 147 (1984).
[27] M. J. Stevens, M. L. Falk, and M. O. Robbins, J. Chem. Phys. **104**, 5209 (1996).
[28] S. Alexander, P. M. Chaikin, P. Grant, G. J. Morales, P. Pincus, and D. Hone, J. Chem. Phys. **80**, 5776 (1984).
[29] L. Belloni (unpublished).
[30] R. D. Groot, J. Chem. Phys. **94**, 5083 (1991).
[31] L. P. Voegtli and C. F. Zukoski, J. Colloid Interface Sci. **141**, 79 (1991).
[32] M. Würth, J. Schwarz, F. Culis, P. Leiderer, and T. Palberg, Phys. Rev. E **52**, 6415 (1995).
[33] T. Palberg, W. Mönch, F. Bitzer, T. Bellini, and R. Piazza, Phys. Rev. Lett. **74**, 4555 (1995).
[34] T. Palberg, J. Kottal, F. Bitzer, R. Simon, M. Würth, and P. Leiderer, J. Colloid Interface Sci. **168**, 85 (1995).
[35] P. M. Chaikin, J. M. di Meglio, W. Dozier, H. M. Lindsay, and D. A. Weitz, in *Physics of Complex and Supramolecular Fluids* (Ref. [4]), p. 65.
[36] M. O. Robbins, K. Kremer, and G. S. Grest, J. Chem. Phys. **88**, 3286 (1988).
[37] U. Apfel, K. D. Hörner, and M. Ballauff, Langmuir **11**, 3401 (1995).
[38] T. Palberg, W. Härtl, U. Wittig, H. Versmold, M. Würth, and E. Simnacher, J. Phys. Chem. **96**, 8180 (1992).
[39] K. Schätzel, W. Weise, A. Sobotta, and M. Drewel, J. Colloid Interface Sci. **143**, 287 (1991).
[40] E. E. Uzgiris, Prog. Surf. Sci. **10**, 53 (1981).
[41] E. Hückel, Phys. Z. **25**, 204 (1924).
[42] M. von Smoluchowski, Bull. Acad. Sci. Cracovie, Classe Sci. Math. Natur **1**, 182 (1903).
[43] A. S. Russel, P. J. Scales, C. S. Mangelsdorf, and S. M. Underwood, Langmuir **11**, 1112 (1995).
[44] R. Krause, B. Dáguanno, J. M. Mendez-Alcaraz, G. Nägele, R. Klein, and R. Weber, J. Phys. Chem. **3**, 4459 (1991).

[45] F. Bitzer, T. Palberg, H. Löwen, R. Simon, and P. Leiderer, Phys. Rev. E **50**, 2821 (1994).
[46] T. Gisler, S. F. Schulz, M. Borkovec, and H. Sticher, J. Chem. Phys. **101**, 9924 (1994).
[47] J. E. Seebergh and J. C. Berg, Colloids Surf., A **100**, 139 (1995).
[48] J. P. H. Zwetsloot and J. C. Leyte, J. Colloid Interface Sci. **163**, 362 (1994).
[49] B. Jönsson, H. Wennerström, P. G. Nilsson, and P. Linse, Colloid Polym. Sci. **264**, 77 (1986).
[50] N. Garbow, J. Müller, K. Schätzel, and T. Palberg, Physica A **235**, 291 (1997).